Kinetics of photoplasma of dense barium vapour

N.I. Kosarev

Abstract. **Barium vapour ionisation under laser photoexcitation of the resonance line at a wavelength of $\lambda = 553.5$ nm is studied numerically. Seed electrons, arising due to the associative ionisation of atoms, gain energy in superelastic collisions and lead to electron avalanche ionisation of the medium. The influence of radiative transfer in a cylindrical gas volume on the excitation kinetics of barium atoms, absorption dynamics of laser radiation and oscillation of ionisation-brightening wave under competition between ionising and quenching collisions of electrons with excited atoms is studied.**

1. Introduction

Paul ion traps are an efficient tool for studying the physics of charged particles in different applications (in particular, classical mass spectrometry [1] and dynamics of high-energy ion beams [2]) and for quantum calculations [3]. In the stage of formation of ionised atoms for their subsequent capture into an ion trap, one must provide efficient ionisation of atoms and increase the concentration of ions. From this point of view, photoionisation of atoms has advantages over other methods (electron–ion emission, thermionic emission, etc.). Much attention is paid to barium sources of ions, obtained by two-photon ionisation [4, 5]. A potential alternative for this method is the formation of barium plasma based on superelastic heating of electrons.

The plasma formed as a result of exposure of a gas to resonant laser radiation is referred to as photoplasma. The problem of photoplasma generation was considered for the first time in [6], where complete ionisation of sodium vapour was experimentally obtained as a result of excitation of the resonant transition in sodium ($\lambda = 589$ nm) by a laser pulse with intensity $I \leqslant 10^6$ W cm^{-2}. The initial atomic concentration was $10^{15}-10^{16}$ cm^{-3}. The results of this experiment [6] were explained in [7–9], and a theoretical model describing the formation of resonant plasma – LIBORS (light ionisation based on resonance saturation) – was developed in [10–13]. Saturation of the resonant transition in a sodium atom ($\lambda=$

N.I. Kosarev Siberian Law Institute, Federal Drug Control Service of Russia, ul. Rokossovskogo 20, 660131 Krasnoyarsk, Russia;
e-mail: kosarev_nikolai@mail.ru

589 nm) by laser radiation leads to associative generation of seed electrons in the medium. Gaining energy in superelastic processes, hot electrons cause avalanche ionisation of sodium atoms and formation of photoplasma.

A computational study of the resonant laser ionisation of optically dense sodium vapor was performed in [14–16]. In regards to barium, the possibility of efficient ionisation of Ba atoms by broadband solar light resulted in its application in the study of open space by means of artificial luminous clouds [17, 18]. Barium vapour injected at altitudes of 160 km or higher is rapidly ionised by solar light and scatters radiation in spectral lines of atoms and ions. The remotely obtained optical data on the atomic and ionised components of barium cloud were used to investigate the physical phenomena and processes occurring in the upper atmosphere and ionosphere of the Earth [17, 18]. The kinetics of photoionisation of barium clouds by solar light was simulated in [19–23].

In this paper, we develop a physicomathematical model of the radiation-collisional kinetics of multilevel barium atoms under laser photoexcitation of the resonant transition with a wavelength of $\lambda = 553.5$ nm. The formation of seed electrons is based on associative ionisation of excited atoms. Numerical solution of the problem makes it possible to investigate the influence of radiative transfer in a cylindrical volume on the excitation kinetics and ionisation of atoms, absorption of laser radiation under conditions of inhomogeneous saturation of the medium, and the dynamics of propagation of ionisation-brightened front under competition between ionising and quenching electron–atom collisions. The method of forming photoplasma based on superelastic heating of electrons may be promising for generating barium ions and studying them in ion traps, because it provides a high efficiency of laser energy conversion into electron energy and, therefore, can be implemented for sufficiently high atomic concentrations at low intensities of laser radiation.

## 2. Model of collisional-radiative kinetics of barium atoms

We consider a cell filled with barium atoms and shaped as a cylinder. A pulsed laser beam with a uniform intensity distribution in the cross section and a frequency coinciding with the frequency of the $^1S_0 \leftrightarrow {}^1P_1$ resonant transition ($\lambda = 553.5$ nm) is incident on one of the end faces of the cell. The pulse duration in the numerical experiment was chosen such as to provide complete ionisation of the gas medium during irradiation at a peak intensity J_0 not higher than 10^3 W cm^{-2} [see τ_p and J_0 in (11)]. For the values used by us (few microseconds), coherent effects were disregarded in the numerical model, because the characteristic times of their manifestation

are much shorter than τ_p and the characteristic times of the process under consideration. The initial atomic concentration N_0, determined from the tables with saturated barium vapour pressures, was varied in the range from 10^{13} to 10^{14} cm^{-3}; this concentration range corresponds to vapour temperatures of 800–820 K. At these temperatures the equilibrium electron concentration is very low; therefore, it was assumed that, before irradiation, the gas consisted of neutral atoms in the ground state.

The number of barium levels taken into account was chosen based on the experience in developing multilevel models for sodium [15, 16] and barium [19–23] atoms. On the one hand, to describe more exactly the plasma formation kinetics, it is desirable to take into account as many levels as possible; on the other hand, an increase in the number of levels significantly increases the number of equations describing the problem [23]. Based on the results of [19–23], an 11-level model of the barium atom (see Fig. 1) was chosen. Specifically, we took into account the ground ($^1S_0$) and excited ($^1P_1^0$) states of the resonant transition (levels 1 and 2 in Fig. 1); metastable $^1D_2$ and $^3D_1$, $^3D_2$, $^3D_3$ states (levels 3–6); a group of four excited levels with the highest oscillator strengths, related to the ground and metastable levels, $6s6p\,^3P_1$, $5d6p\,^1D_2$, $5d6p\,^1P_1$, and $6s7p\,^1P_1$ (levels 7–10); and the ionised state.
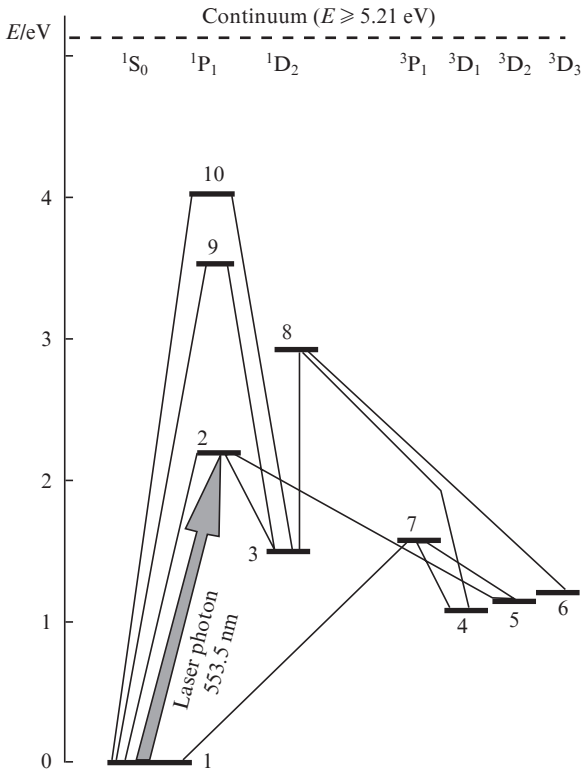
Figure 1. Schematic diagram of the energy levels of barium atom that are used in the model. A number near a level is its serial number in the balance equations; lines indicate spontaneous decay from higher to lower level.

The kinetics of atomic levels was described by the rate population balance equations, taking into account the following elementary processes: excitation and quenching of the resonant state by laser radiation and spontaneous decay of resonant and other excited states (the directions of spontaneous decay are indicated by lines in Fig. 1); associative ionisa-

tion of the excited $^1P_1^0$ level; electron-impact excitation, relaxation and ionisation of atoms; and photo- and three-particle recombinations of barium ion. The mechanism of formation of seed electrons in barium vapour should be discussed. The associative ionisation cross section for the $^1P_1^0$ level of the barium atom was reported to be $Q_a(^1P_1^0 + {}^1P_1^0) = 1\times10^{-13}$ cm^2 in [24]. The data on the Penning ionisation cross sections for several groups of atomic levels in barium can be found in [25]. Since the rate of increase in the seed-electron concentration in balance equations is determined by the product of the cross section on the concentrations of atoms in the corresponding states, the Penning mechanism should be taken into account for the pairs of levels containing the $^1P_1^0$ level. This level is populated under laser irradiation. Therefore, according to [25], the only process responsible for seeding is the Penning ionisation with participation of the $^1P_1^0$ and $^3D_1$ states with the cross section $Q_p(^1P_1^0 + {}^3D_1) = 7\times10^{-13}$ cm^2 (levels 2 and 4 in Fig. 1). The cross section Q_p exceeds several times Q_a; however, the $^3D_1$ level is not related to the $^1P_1^0$ state in the dipole approximation. Therefore, the population of the $^3D_1$ level in the initial stage of excitation of barium resonant level by laser field is close to zero. In view of this, the Penning ionisation mechanism can be neglected. Numerical calculations were performed taking into account only associative ($^1P_1^0 + {}^1P_1^0$) or Penning ($^1P_1^0 + {}^3D_1$) electrons. The test results confirmed the exclusive effect of the associative mechanism for generating electrons with participation of the excited $^1P_1^0$ state.

With allowance for the aforementioned processes, the kinetics equations for the populations of atomic states at a specified point r of the medium at an instant t, along with the equation for the electron concentration N_e, take the form

$$\frac{\partial N_1}{\partial t} = -P_{12}N_1 + P_{21}N_2 + \sum_{i=2}^{10} A_{i1}N_i$$
$$+ \sum_{\substack{i\neq1}}^{10}(K_{i1}N_i - K_{1i}N_1)N_e + R_1N_e^3 - S_1N_1N_e + F_1N_e^2, \quad (1)$$

$$\frac{\partial N_2}{\partial t} = P_{12}N_1 - P_{21}N_2 + \sum_{i=3}^{10} A_{i1}N_i - A_{21}N_2$$
$$+ \sum_{\substack{i\neq2}}^{10}(K_{i2}N_i - K_{2i}N_2)N_e + R_2N_e^3$$
$$- S_2N_2N_e + F_2N_e^2 - \alpha_a N_2^2, \quad (2)$$

$$\frac{\partial N_m}{\partial t} = \sum_{i>m} A_{im}N_i - \sum_{i<m} A_{mi}N_m + \sum_{i\neq m}(K_{im}N_i - K_{mi}N_m)N_e$$
$$+ R_mN_e^3 - S_mN_mN_e + F_mN_e^2, \quad (3)$$

$$m = 3, 4, ..., 10, \quad i = 1, 2, ..., 10,$$

$$\frac{\partial N_e}{\partial t} = \sum_{i=1}^{10}(S_iN_iN_e - R_iN_e^3 - F_iN_e^3) + \alpha_a N_2^2. \quad (4)$$

Here, $N_m(r,t)$ is the concentration of atoms in the mth state; $N_e(r,t)$ is the electron concentration; A_{im} ($i > m$) are the Einstein coefficients for spontaneous emission; $P_{12} = B_{12}J(r,t)$ and $P_{21} = B_{21}J(r,t) + A_{21}$ are, respectively, the frequencies of

radiative photoexcitation of the ground level (1) and optical quenching of the excited level (2), in which B_{12} and B_{21} are, respectively, the Einstein coefficients for absorption and spontaneous emission; $J(r,t)$ is the integrated (over solid angle and frequency) radiation intensity in the medium at a point r at an instant t; K_{mi} and K_{im} are, respectively, the coefficients of electron excitation and relaxation of levels (the former were calculated within the Born approximation [26], while the latter were calculated using the detailed equilibrium condition); S_m are the electron-impact ionisation coefficients of atoms from the corresponding states m, calculated from the Lotz formula [26]; R_m are the constants of three-particle electron–ion recombination rates, calculated from the detailed equilibrium condition; F_m are the electron–ion photorecombination coefficients, determined according to the technique of [27]; and α_a is the constant of associative ionisation rate.

At the initial instant ($t = 0$), all atoms are in the ground state with a concentration N_0. Therefore, the initial conditions for Eqns (1)–(3) can be written as

$$N_1(r,0) = N_0, \ N_m(r,0) = 0, \ m = 2, 3, ..., 10.$$

The kinetics equations for a multilevel atom should be supplemented with the equation for electron temperature T_e; for T_e measured in electronvolts, this equation takes the form

$$\frac{\partial T_e}{\partial t} = \frac{2}{3}\sum_{i>k}^{10}(K_{ik}N_i - K_{ki}N_k)\Delta E_{ki} + \sum_{i=1}^{10}\left(\frac{2}{3}I_i + T_e\right)(R_iN_e^2 - S_iN_i)$$

$$- \frac{2}{3}H_{ea}\sum_{i=1}^{10}N_i - \frac{2}{3}H_{ei}N_e, \tag{5}$$

where I_i are the ionisation potentials of the corresponding atomic levels; ΔE_{ki} is the energy difference between the kth and ith levels (in eV); and H_{ea} and H_{ei} are the energy transfer rates in elastic collisions of electrons with atoms and ions [10–13].

The initial conditions for Eqns (4) and (5) are as follows:

$$N_e(r,0) = 0, \ \ T_e(r,0) = T_e^0.$$

Here, T_e^0 is the initial temperature of the electrons formed as a result of associative ionisation of barium atoms.

Note that Eqn (5) does not take into account the rate coefficient of electron energy accumulation as a result of inverse bremsstrahlung absorption Q_{br}, which has, according to the estimates of [14], the form:

$$Q_{br} \approx \frac{10^{-7}N_0^2\lambda^2 I}{12c^2 T_e^{3/2}},$$

where $N_e = N_0/2$; λ is the radiation wavelength (in cm), T_e is the temperature (in eV) and I is the intensity (in W cm^{-2}). The energy of the electron accumulation rate in superelastic collisions can be written as

$$Q_{sc} \approx \frac{g_2}{g_1 + g_2}\frac{N_0^2}{4}K_{21}\Delta E_{21},$$

where g_1 and g_2 are the statistical weights of states 1 and 2 and ΔE_{21} is the energy-level difference for the barium resonant line. It can be shown that Q_{br} and Q_{sc} become equal at $I \approx$

10^{11} W cm^{-2}. In our case, $I \approx 10^3$ W cm^{-2}; therefore, the bremsstrahlung absorption can be neglected in the model.

The laser radiation absorption and transfer in a three-dimensional gas volume are taken into account in Eqns (1) and (2) via factors P_{12} and P_{21}, in which

$$J(r,t) = \int_0^{2\pi}d\varphi\int_0^\pi\sin\theta\,d\theta\int_0^\infty\Phi(x)I(r,\theta,\varphi,x,t)dv. \tag{6}$$

Here,

$$\Phi(x) = \frac{1}{\sqrt{\pi}}\exp(-x^2)$$

is the normalised contour of absorption line, formed by Doppler broadening; $x = (v - v_0)/\Delta v_D$ is a dimensionless frequency; v_0 is the central frequency of the spectral line; and Δv_D is its Doppler width. The propagation of radiation with intensity $I(r,\theta,\varphi,x,t)$ at a frequency x in the direction determined by angles θ and φ, at a spatial point $r(x,y,z)$ of three-dimensional volume, is described by the transfer equation

$$\frac{\partial I(r,\theta,\varphi,x,t)}{\partial l} = \Phi(x)\chi_0(N_1,N_2)[S(N_1,N_2) - I(r,\theta,\varphi,x,t)]. \tag{7}$$

We used its stationary form, because the laser beam velocity in a medium greatly exceeds the rate of change in the parameters of the medium. Here, ∂l is a small increment in the photon path in the direction L; χ_0 is the absorption coefficient at the line centre, and S is the source function. With allowance for the normalisation of contour $\Phi(x)$ and S, we have

$$\chi_0(N_1,N_2) = \frac{c^2 A_{21}g_2}{8\pi v_0^2 g_1\Delta v_D}\left[N_1 - \frac{g_1}{g_2}N_2\right],$$

$$\tag{8}$$

$$S(N_1,N_2) = \frac{2hv_0^3 g_1}{c^2 g_2}\frac{N_2}{N_1 - (g_1/g_2)N_2},$$

where c is the speed of light and h is Planck's constant.

The laser beam has a radially symmetric distribution of intensity in the cross section and is incident at a right angle to the left end face of the cylinder of height H_0. Therefore, the boundary condition for (7) at the left boundary ($z = -H_0/2$) has the form

$$J(r(z=-H_0/2),\theta,\varphi,x,t) = \begin{cases} 0 \text{ at } \theta \neq 0, \\ J_{las}(R,x,t) \text{ at } \theta = 0, \end{cases} \tag{9}$$

where R is the radial coordinate. There is no incident radiation at the right boundary of the cylinder ($z = H_0/2$), and, for $\theta \geqslant 90°$, we have zero boundary conditions in the form

$$J(r(z=-H_0/2),\theta,\varphi,x,t) = 0, \tag{10}$$

where the variable θ is the angle between the direction of the scattered photon and the symmetry axis z of the cylinder. The shape of the laser pulse is set as follows:

$$J_{las}(R,x,t) = J_0\frac{(\Delta x_{las}/2)^2}{x^2 + (\Delta x_{las}/2)^2}\frac{t}{\tau_p}\exp\left(1 - \frac{t}{\tau_p}\right)F(R). \tag{11}$$

Here, $F(R)$ sets a dependence of the laser radiation intensity in the beam cross section on the radial coordinate R; τ_p is the time during which the pulse intensity reaches the peak value

J_0; and Δx_{las} is the width (measured in $\Delta \nu_D$ units) of the lasing spectrum, which has a Lorentzian dependence on frequency.

Equations (1)–(11) form a closed system of integro-differential equations. Their numerical solution, with allowance for the radiative transfer in a cylindrically symmetric volume, was performed based on the methods developed in [14, 23]. We calculated the population kinetics of multilevel atoms, electron temperature and density, and the frequency–angular characteristics of vapour-scattered radiation at any specified instant. Below we report the results of simulating the plasma formation kinetics in barium vapour.

3. Kinetics of photoplasma of barium atoms

The computational study of plasma formation kinetics was performed for different model parameters (initial concentrations of barium atoms, intensity and duration of laser irradiation and distribution of laser radiation intensity in the beam cross section). We analysed the results obtained for the uniform laser intensity distribution in the beam cross section for a cylinder with a height $H_0 = 1.0$ cm and a radius $R_0 = 0.5$ cm. Figure 2 shows time dependences of the electron concentration N_e and electron temperature T_e (averaged over the cylinder height) and the populations of the ground ($^1S_0$) and excited ($^1P_1^0$) states of the resonant transition of barium atom [curves (1), (2)] and metastable ($^3D_1$ and $^3D_2$) levels [curves (3), (4)]. The optical density of the medium, τ_0, calculated based on the cylinder diameter according to the expression $\tau_0 = \chi_0 2R_0$ (at the initial concentration of barium atoms $N_0 = 6.13\times10^{13}$ cm^{-3}), turned out to be 4000. Under these conditions, the laser radiation intensity $I_0 = 10^3$ W cm^{-2} is insufficient for saturating the entire volume of irradiated vapour, and the significant fraction of radiation is absorbed by barium atoms [Fig. 3, curve (2)]. The saturation intensity (with radiation trapping neglected) can be equated to power I_{sc}, scattered by unit surface area of pumped volume with a height $H_0 = 1$ cm [28].

Substituting the values $A_{21} = 1.19\times10^8$ s^{-1} and $h\nu$ for the resonant transition into this expression, we obtain $I_{sc} = 4.3\times10^{-11}\cdot N_2$ W cm^{-2}. Under close-to-saturation conditions, the population of the excited level is related to the initial atomic concentration by the expression

$$N_2 = g_2/(g_1 + g_2)N_0. \tag{12}$$

With allowance for (12), at $N_0 = 6.13\times10^{13}$ cm^{-3}, we obtain the pump intensity $I_p \approx 2\times10^3$ Wcm^{-2}. Actually, when laser radiation is absorbed and scattered in optically dense media, the real saturation intensity may exceed I_{sc} by three orders of magnitude [28]. Therefore, the pumped volume with barium atoms is not completely saturated at an intensity $I_0 = 10^3$ W cm^{-2}.

Three radically different regimes can be selected in the evolution of ionisation brightening of barium vapour (Fig. 2). The first regime corresponds to the initial stage of irradiation of medium by a laser beam, when Ba atoms are redistributed (for a time of ~0.5 µs) between the ground [curve (1)] and metastable states via the excited $^1P_1^0$ level [curve (2)] as a result of radiative excitation and spontaneous decay. The $^3D_2$ level [curve (4)] is characterised by the highest population: the probability of spontaneous decay to this level from the $^1P_1^0$ level exceeds the decay probability to other metastable levels. For this reason, the populations of the metastable $^1D_2$ and $^3D_3$ levels are much lower than the populations of the $^3D_1$ and $^3D_2$ levels; their temporal evolution is not shown in Fig. 2. For the same time (0.5 µs), the electrons arising in the medium due to the associative mechanism, are heated in superelastic processes, and their temperature reaches the peak value $T_e^{max} = 1.66$ eV (the dashed line).

If the metastable $^3D_2$ level is populated simultaneously with photoexcitation of the $^1P_1^0$ state, the increase in the population of the metastable $^3D_1$ level [curve (3)] is delayed in time. In addition, the beginning of rise in the population of the $^3D_1$ level coincides with the increase in the electron concentration (Fig. 2, dashed line). This fact suggests that this level is occupied mainly via relaxation of the $^3P_1$ level, while the latter is occupied, in particular, due to the collisions of electrons with atoms in the ground state $^1S_0$. After reaching the value $T_e^{max} = 1.66$ eV, the temperature begins to decrease due to the inelastic collisions between atoms and electrons, as a result of which the latter lose energy and are cooled.

The next regime of ionisation development is characterised by the state in which the level populations and electron concentration change not so rapidly as in the first regime (2–5 µs, Fig. 2). Here, atoms on the irradiated end face of the gas cell start being partially ionised under electron impact, because the electron concentration is still increasing. Deep in the cylindrical cell, closer to its shadow end face, the ionisation development is still very weak because of the strong absorption of laser radiation by barium vapour. In this regime of low saturation of the medium by the laser field, the populations of levels of a multilevel atom are characterised by significant spatial and temporal inhomogeneities [14–16].

In the third regime of ionisation brightening of barium vapour, the electron-impact ionisation of barium atoms comes to end. For the model parameters corresponding to Fig. 2, this regime begins at times not shorter than 5 µs and is characterised by a decrease in the populations of all levels of barium atom (the ground and excited levels of the resonant transition and all other excited and metastable states). Finally, the electron concentration reaches a value equal to the initial atomic concentration in the medium ($N_e/N_0 \approx 1$). Therefore, the laser-irradiated gas volume is completely ionised at the end of the time interval under consideration. Hence, the elec-
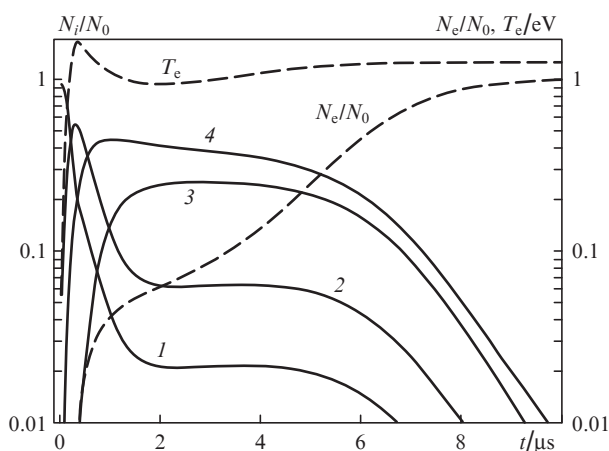
Figure 2. Time dependences of the electron concentration N_e and electron temperature T_e and the populations of atoms in the (1) $^1S_0$, (2) $^1P_1^0$, (3) $^3D_1$, and (4) $^3D_2$ states, averaged over the cylinder height H_0, at $N_0 = 6.13\times10^{13}$ cm^{-3}, $\tau_p = 3$ µs, $\Delta x_{las} = 4\Delta \nu_D$, $J_0 = 10^3$ W cm^{-2}, and $\tau_0 = 4000$. The ordinate axis is on the log scale.

tron temperature, after a small decrease in the previous stage of ionisation evolution, becomes quasi-steady-state and approaches 1.24 eV. This value is determined by the balance between forward and backward excitation collisions between electrons and atoms even in the stage of formation of electron-impact avalanche ionisation of atoms.

Complete ionisation of barium atoms leads to brightening of the medium, because the latter does not contain any absorbing atoms. As a result, the laser beam passes through the barium vapour almost without absorption. The laser pulse absorption dynamics is shown in Fig. 3, which presents time dependences of the laser radiation transmittance through barium vapour at different initial atomic concentrations. Curve (2) corresponds to the same model parameters as in Fig. 2; at these parameters the avalanche ionisation develops for a fairly long time (more than 7 μs). An increase in the initial atomic concentration in the volume (with the laser intensity and pulse duration retained the same), the electron avalanche ionisation develops more rapidly [curve (3)]. The reason is that the rate of increase in the electron concentration via the associative mechanism is proportional to the second power of the excited-atom concentration. Therefore, an increase in N_0 in the medium enhances the development of the electron avalanche ionisation of barium atoms. If the initial atomic concentration is reduced from 6.13×10^{13} to 4.59×10^{13} cm^{-3}, the electron-impact ionisation cannot be developed during the time of pulse duration [Fig. 3, curve (1)]. In this case, the transmittance monotonically decreases due to a decrease in the laser pulse intensity.
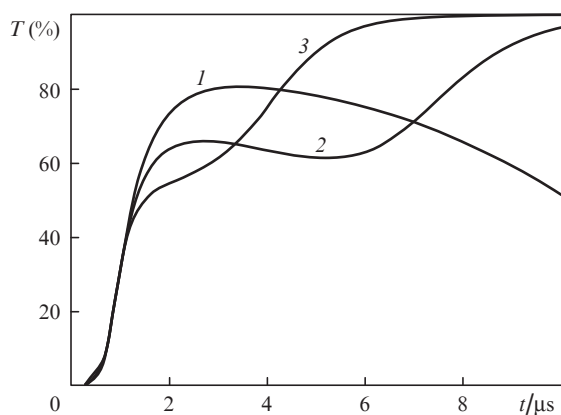
Figure 3. Dynamics of transmittance T (the ratio of the frequency-integrated intensity of the laser radiation transmitted through barium vapour to the input intensity) for the initial atomic concentrations $N_0 =$ (1) 4.59×10^{13}, (2) 6.13×10^{13}, and (3) 7.68×10^{13} cm^{-3}. The laser radiation parameters are the same as in Fig. 2.

Let us consider curve (2) in Fig. 3. In contrast to curve (3), this dependence does not demonstrate a monotonic increase in the laser radiation transmittance during development of avalanche ionisation. The behaviour of curve (2) indicates that strong absorption of laser radiation occurs in the second regime of development of barium vapour ionisation. The transmittance reaches a maximum value at $t = 2$ μs, after which begins to decrease. This fact is indicative of an increase in the laser radiation absorption by vapour. An increase in the electron concentration gives rise to the transient regime of avalanche electron ionisation of atoms. In the beginning of this process, the medium becomes optically

denser (grows 'turbid'), because the excited state of barium atom is quenched by electrons. The effect of optical darkening was predicted for the first time in [8, 9], where it was shown that two regimes can be implemented under irradiation of a gas medium by resonant radiation.

First, when a close-to-saturation state is implemented, the populations of resonant levels are equalised, and seed electrons are formed via the associative mechanism. Their energy is stabilised, and the further increase in the electron concentration is due to the electron collisional ionisation of atoms. With an increase in the electron concentration, when the rate of quenching electronic processes exceeds the impact ionisation rate, the laser radiation is absorbed more intensively because of the increase in the absorption coefficient of the medium. The second regime is implemented when the electron-impact ionisation rate exceeds the collisional quenching rate, as a result of which the medium is brightened. The increase in the laser radiation absorption leads to the formation of an ionisation wave on the irradiated surface of the vapour volume. This wave propagates into the bulk of the medium, causing its additional brightening. Under these conditions, the initially neutral gas becomes completely ionised. The effect predicted in [8, 9] was confirmed by computation for sodium vapour in [15, 16], where darkening was clearly observed for sodium vapour pumped by a laser beam with $\lambda = 589.6$ nm.

In particular, the laser pulse was divided into two subpulses: one preceding the onset of avalanche ionisation, when quenching electronic collisions dominate over ionising, and the other following the development of electron avalanche ionisation, after brightening the gas volume. This effect is also observed for barium vapour; however, it is less pronounced, and the laser pulse intensity in maximum obeys the relation $I_0 \leqslant 10^3$ W cm^{-2}. The main reason for this is as follows. The sodium atom has no metastable states optically related to excited levels of resonant transitions with wavelengths of 589.6 or 589 nm; therefore, when any of these resonant levels is photoexcited by the laser field, there is no reservoir of an additional radiative drain of particles for them. When the excited state is quenched by electrons in the transient regime directly before the development of avalanche ionisation, sodium atoms relax to the ground state. Correspondingly, the increase in its population leads to a decrease in the concentration of excited atoms and a significant increase in the absorption coefficient χ_0 [see (8)]. The presence of the metastable levels related to the excited $^1\mathrm{P}_1^0$ state in the barium atom makes atoms be redistributed from the excited state to these metastable levels. Therefore, the electron-induced quenching of the excited $^1\mathrm{P}_1^0$ state, as well of all other levels excited by direct electron–atom collisions, does not lead to any significant increase in the absorption coefficient at the resonant transition in barium with a wavelength $\lambda = 553.5$ nm. Specifically this circumstance determines the so small decrease in transmittance in Fig. 3 [curve (2)].

These results indicate the following: with an increase in the degree of ionisation, the laser beam front moves forward, towards the shadow end face of the cylinder. When the medium 'darkens', the laser beam front, vice versa, moves back to the irradiated end face. However, the degree of ionisation continues to increase, the medium brightens again and the laser beam front moves again toward the shadow end face of the cylinder. Now it can be considered as the ionisation brightening front. As this front advances, a saturation region is formed in its head, due to which processes of electron-

impact ionisation of atoms are developed in this region. This effect (oscillation of the front of ionisation-brightened region) was also obtained numerically for sodium vapour [15, 16]. For the aforementioned reasons, it is less pronounced for barium.

As was indicated in Section 2, the constructed model takes into account the processes of resonant radiation transfer. When laser radiation is absorbed, barium atoms rescatter photons into the environment, as a result of which the local values of both the source function and the absorption coefficient change. Within the absorbing volume, the re-emitted photons are immediately absorbed by atoms, while near its boundary radiation may leave the medium, thus violating the balance of direct and inverse radiative and collisional processes. Due to the escape of radiation through the gas-volume boundary, relaxation of excited barium atoms and, as a consequence, significant cooling of electrons occur near this boundary. In this way, the rescattered radiation affects (via the source function) the level occupation kinetics during plasma formation.

Figure 4 demonstrates the role of radiative-transfer effects in dense barium vapour: it shows the spatial distributions of
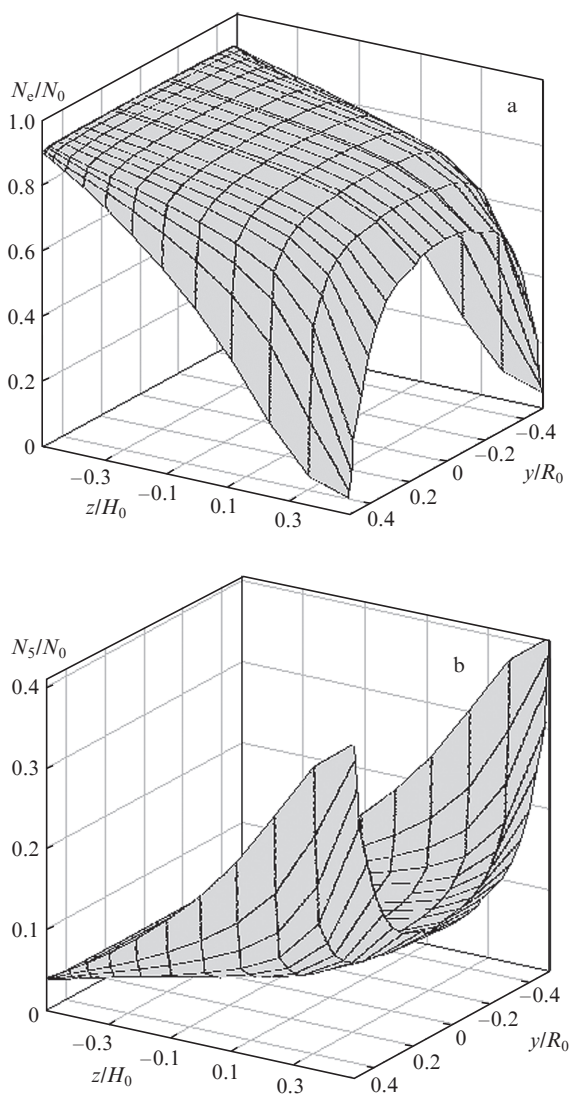
Figure 4. Spatial distributions of (a) electron concentration and (b) population of the metastable $^3D_2$ state at the instant $t = 8.0$ μs. The model parameters are the same as in Fig. 2.

electron concentration and population of the metastable $^3D_2$ state at the instant $t = 8$ μs. It is noteworthy that the degree of ionisation on the irradiated boundary of the medium reaches 90%. At the same time, the degree of ionisation is about 60% on the shadow end face of the cylinder (in the centre of the face) and hardly reaches 5% on the lateral boundary. As was noted above, this inhomogeneous spatial distribution of the electron concentration is explained by radiative-transfer processes, because the escape of radiation through the cylinder surface leads to relaxation of excited atoms and cooling of the electrons gaining energy in superelastic collisions. As follows from the shape of the surface (Fig. 4b), the radiative transfer at the resonant transition of barium atom with $\lambda = 553.5$ nm leads to a highly inhomogeneous occupation of the metastable $^3D_2$ state. In addition, since this level has a high population, its contribution to electron concentration is about 35%.

4. Main results and conclusions

The main results of our study are as follows.

(i) The Penning and associative mechanisms of generation of seed electrons for barium atom were analysed by using the data on the cross sections of these processes. Our estimates showed that, under a laser effect on the resonant transition with $\lambda = 553.5$ nm, the dominant mechanism of their generation is associative ionisation.

(ii) A collisional-radiative model is developed, which describes the kinetics of excitation and ionisation of barium atoms with allowance for the radiative transfer at the resonant atomic line ($\lambda = 553.5$ nm). The numerical method for solving the obtained system of integro-differential equations, developed for the cylindrical geometry of the gas medium, makes it possible to obtain a spatial and temporal pattern of laser radiation absorption, population kinetics of atomic levels, the electron concentration and temperature, and the dynamics of frequency–angular distribution of radiation scattered by vapour for any specified point of three-dimensional volume.

(iii) It is found that, after excitation by resonant radiation with $\lambda = 553.5$ nm, the population of the $^1P_1$ level decreases because of the redistribution of atoms over metastable states. The population of the metastable $^3D_2$ level exceeds (due to the spontaneous relaxation of the excited $^1P_1^0$ level) the populations of other levels. The population of the $^3D_1$ level is lower than that of the $^3D_2$ state by a factor of almost 2; it is formed mainly according to the collisional mechanism through relaxation of the $^3P_1$ state.

(iv) In the case of spatially inhomogeneous saturation of the resonant transition, the electron avalanche ionisation of atoms begins on the irradiated end face of the cylinder. The ionisation-brightened front begins to propagate into the bulk of the medium, causing its additional brightening. Then an additional energy-loss channel (related to superelastic quenching of resonant atoms) arises, and the medium becomes optically denser. Darkening of the medium causes backward motion of the laser intensity front to the irradiated end face of the cylinder. Further development of the electron avalanche ionisation of barium restores the propagation of the brightened region into the bulk of the gas medium. When the atoms are completely ionised, the laser radiation is hardly absorbed because the absorption coefficient is small. The fact that the laser energy is less absorbed as a result of ionisation of the medium can be used to reduce the energy loss in the problems of efficient transfer of laser radiation energy through resonantly absorbing media.

(v) Radiative transfer in a cylindrical volume causes a highly nonuniform spatial distribution of the concentration of excited atoms and, as a consequence, electron concentration. Inside a gas-filled cell (closer to its symmetry axis), trapping of resonant photons plays an important role. Therefore, the concentration of atoms in all excited states is higher and the electron temperature and concentration are much higher in this region than at the boundaries of the medium, where escape of photons from the cell leads to relaxation of excited state and reduces the degree of ionisation. This spatial separation of charges along the optical-excitation axis leads to the generation of photo emf; this effect was observed experimentally in [29].

To conclude, we should note that the method of forming barium photoplasma, based on the mechanism of heating electrons in superelastic processes, may be an alternative way of generating ions in high concentrations for ion traps.

References

1. Paul W. *Rev. Mod. Phys.*, **62**, 531 (1990).
2. Gilson E.P., Davidson R.C., Efthimion P.C., Majeski R. *Phys. Rev. Lett.*, **92**, 155002 (2004).
3. Freidenauer A., Schmitz H., Glueckert J.T., Porras D., Schaetz T. *Nature Phys.*, **4** (10), 757 (2008).
4. Steele A.V., Churchill L.R., Griffin P.F., Chapman M.S. *Phys. Rev. A*, **75** (5), 053404 (2007).
5. Wang B., Zhang J.W., Gao C., Wang L.J. *Opt. Express*, **19** (17), 16438 (2011).
6. Lucatorto T.B., McIlrath T.J. *Phys. Rev. Lett.*, **37** (7), 428 (1976).
7. Measures R.M. *J. Appl. Phys.*, **48**, 2673 (1977).
8. Shaparev N.Ya., in: *Abstracts of Fourth Europhysics Sectional Conf. on Atomic and Molecular Physics of Ionized Gases* (Essen, Germany, 1978) Pt. 48.
9. Shaparev N.Ya. *Zh. Tekh. Fiz.*, **49**, 2223 (1979).
10. Measures R.M., Drewell N., Cardinal P. *J. Appl. Phys.*, **50** (4), 2662 (1979).
11. Measures R.M., Cardinal P.G., Schinn G.W. *J. Appl. Phys.*, **52** (3), 1269 (1981).
12. Measures R.M., Cardinal P.G. *Phys. Rev. A*, **23** (2), 804 (1981).
13. Measures R.M., Wong S.K., Cardinal P.G. *J. Appl. Phys.*, **53** (8), 5541 (1982).
14. Kosarev N.I. *Mat. Model.*, **17** (5), 105 (2005).
15. Kosarev N.I., Shaparev N.Ya. *Opt. Atmos. Okeana*, **19** (2–3), 216 (2006).
16. Kosarev N.I., Shaparev N.Ya. *Kvantovaya Elektron.*, **36** (4), 369 (2006) [*Quantum Electron.*, **36** (4), 369 (2006)].
17. Rosenberg N.W., Best G.T. *J. Phys. Chem.*, **75**, 1412 (1971).
18. Bernhardt P.A., Roussel-Dupre R.A., Pongratz M.B., et al. *J. Geophys. Res.*, **92**, 5777 (1987).
19. Shaparev N.Ya., Shkedov I.M. *Opt. Atmos. Okeana*, **4** (11), 1175 (1991).
20. Kosarev N.I., Shkedov I.M. *Opt. Atmos. Okeana*, **4** (11), 1169 (1991).
21. Kosarev N.I., Shkedov I.M. *Opt. Atmos. Okeana*, **6** (10), 1298 (1993).
22. Kosarev N.I., Shkedov I.M. *Opt. Atmos. Okeana*, **12** (1), 30 (1999).
23. Kosarev N.I. *Mat. Model.*, **18** (12), 67 (2006).
24. Kallenbach A., Kock M., Zierer G. *Phys. Rev.*, **38** (5), 2356 (1988).
25. Kallenbach A., Kock M. *J. Phys. B: Atom. Molec. Phys.*, **22**, 1705 (1989).
26. Sobel'man I.I., Vainshtein L.A., Yukov E.A. *Excitation of Atoms And Broadening of Spectral Lines* (Berlin: Springer-Verlag, 1995; Moscow: Nauka, 1979).
27. Sobel'man I.I. *Introduction to The Theory of Atomic Spectra* (Oxford: Pergamon, 1972; Moscow: Nauka, 1977).
28. Kosarev N.I. *Opt. Spektrosk.*, **101** (1), 64 (2006).
29. Gorbunov N.A., Stacewicz T. *Pis'ma Zh. Tekh. Fiz.*, **26** (15), 21 (2000).